2021 IEEE International Conference on Systems, Man, and Cybernetics (SMC)
17-20 October, 2021. Melbourne, Australia

Kinematically Admissible Editing of the Measured Sensor Motion Data for Virtual Reconstruction of Plausible Human Movements

Adithya Balasubramanyam[1], Ashok Kumar Patil[2], Bharatesh Chakravarthi[2], Jaeyeong Ryu[2] and Young Ho Chai[2]

***Abstract*— Sensor acquired data from inertial measurement unit based motion capture systems often do not conform to human body kinematics. Although the data may appear visually correct when reconstructed on a stick model or 3D avatar, it does not represent natural movement when visualized on 3D data analytical tools, such as Motion-sphere. This work extends the Motion-Sphere human motion data visualization and analysis tool to edit sensor acquired human motion data (SHMD) to strictly adhere to human body kinematics. We use knee and elbow joint movements from the range of motion data in the TotalCapture dataset to compare SHMD against edited human motion data. This work proposes a method to edit SHMD using Motion Sphere for kinematic correctness. We verify that edited human motion data is admissible to human body kinematics and improves virtual reconstruction on 3D avatar and joint position estimation accuracy. Our results highlight the requirement for data visualization and editing tools, such as Motion-sphere to edit and clean SHMD.**

I. INTRODUCTION

This study's primary objective was to process sensor acquired human motion data (SHMD) for consistency, accuracy, and correctness. Inertial measurement unit (IMU) based motion tracking has received considerable research attention, since many applications require accurate tracking conforming to human body kinematics [1], [2], [3], [4]. It is challenging to calculate human joints rotations with IMU sensors strapped to the body, e.g. Cheng et.al. [5] attached IMUs to the body at strategic locations to capture bone segment orientation as quaternions. The challenge is to align IMU and bone segment data to the sensor's coordinate frame, and generally some form of calibration procedures addresses this issue before motion capture. Some studies [6], [7] make the subjects stand in a pre-defined still pose to achieve meaningful alignment between bone-segments and sensors.

Since IMUs measure the orientation for the rigid body they are attached to, a separate procedure is followed to establish the kinematic link between bone segments [8], [9]. The procedure first defines parent-child relationships between individual bone segments, and then derives quaternion transformations to determine actual rotation required for accurate reconstruction on a 3D avatar.

However, most contemporary sensors are designed to measure attitude and position with 6 degrees of freedom (DoFs) [8]. Therefore, IMUs will always yield non-zero values in the three rotational DoFs regardless of the calibration, inevitably contributing to position and orientation error [10]. Figure 1 shows lower leg rotation about the knee joint. The knee is essentially a hinge joint with a single rotational DoF. The data is visualized on Motion-sphere, a human motion visualization tool [11]. Motion-sphere can visually magnify subtle human motion by decomposing rotations into twist and swing, and then representing them as series of quaternions on a unit sphere. Color coded miniature 3D models or beads represent a single quaternion frame. Therefore, Motion-sphere can visualize twist and swing rotation for individual bone segments on the human body relative to the parent bone in accordance with kinematic hierarchy (Fig. 1(a))

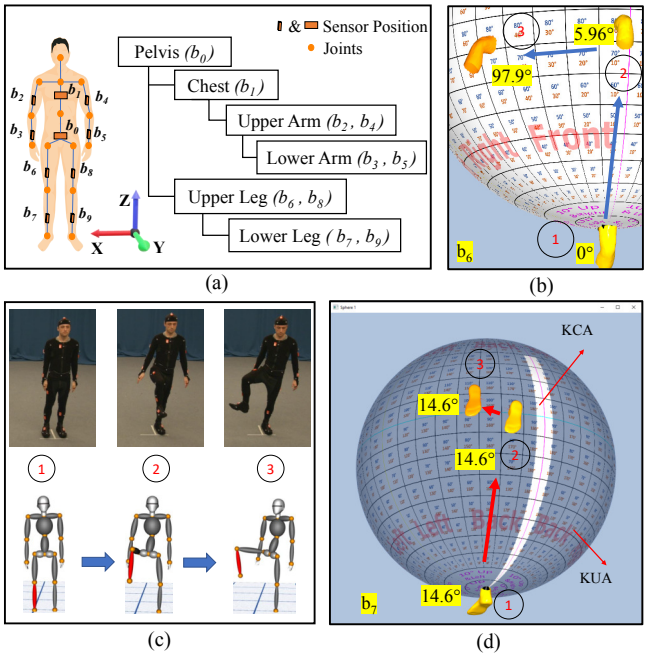

Fig. 1. (a) Kinematic hierarchy considered in this work, (b) key frames visualized on Motion-sphere for the right upper leg (b_6), (c) key frames from TotalCapture [16] range of motion data, (d) key frames visualized on Motion-sphere for the right lower leg (b_7). Highlighted area indicate constrained area and darkened area indicate un-constrained area.

Figure 1(a) shows how sensor acquired human motion data from IMUs attached to the upper and lower legs; collectively determine lower leg orientation in a kinematic chain. Although SHMD reconstruction on a 3D virtual avatar is visually accurate (Fig. 1(c)), visualizing SHMD in a visual motion analytic tool, such as Motion-sphere, tells a different

[1]Dept of Computer Science and Engineering, PES University, Bengaluru, India, adithyab@pes.edu
[2]GSAIM, Chung Ang University, Seoul, South Korea, yhchai@cau.ac.kr

978-1-6654-4207-7/21/$31.00 ©2021 IEEE

story. Figure 1(d) shows that the lower leg should rotate with a single rotational DoF within a kinematic constrained area (KCA) on the sphere, but the data exhibits a three DoF rotation in kinematic unconstrained area (KUA). This anomaly is ignored largely by most current motion capture systems [12], [13], [14], [15].

However, the SHMD is treated as a valuable data throughout the current work. It is the correction of the SHMD with respect to kinematics of human body, that the current work deals with. Therefore, no data is clipped, omitted or added as part of the editing process. This study extends Motion-sphere to human motion editing and authoring, by allowing SHMD issues concerning kinematic constraints to be edited for consistency, accuracy, and correctness. Experimental results confirmed that this edited human motion data (EHMD) is consistent with human kinematics and improves joint and bone segment positional and orientation estimation accuracy. The 3D avatar used to reconstruct human motion is a combination of multiple parametric ellipsoids, and hence EHMD twist changes are not visually noticeable in the virtual reconstruction. However, Motion-sphere representation highlights twist using color coded miniature 3D models.

The proposed work demonstrates problems with publicly available IMU based motion capture data, i.e., the TotalCapture data set [16], using Motion-sphere visualization. We compared joint and segment orientation and position with ground truth after editing the data for kinematic correctness. Due to the kinematic correctness in the EHMD, the data finds usage in many applications including motion authoring, motion analysis, accurate pose detection, and activity recognition systems. Kinematic correctness of the motion data plays an important role in activity recognition [17]

II. RELATED WORK

Wang et al. [18] categorize 3D motion editing and synthesis into four classes: manual, physics, video, and motion capture approaches. The current study considers motion capture editing, hence this section discusses previous studies that synthesize EHMD from SHMD.

Kovar et al. [19] proposed an algorithm to edit SHMD to solve foot skate problems. Their algorithm modified orientation and position for all joints except end effectors. EHMD assumes single DoF for knee joints, leaving SHMD unchanged for data that was not directly edited. Their method not only adjusted orientation and position but also gracefully changed bone segment length to eliminate artifacts. Their objective was smooth and natural looking animation for the stick model that was later reconstructed on a 3D virtual avatar.

Key frame selection is crucial since they can influence artifacts introduced in the resulting EHMD, and data are commonly interpolated between specific key frames. Interpolation cannot be fully eliminated since motion capture systems already generate enormous data volumes. Lee and Shin [20] proposed a technique to adapt SHMD with specific constraints and incorporated hierarchical curve fitting and inverse kinematic solver to synthesis desired motion. Their data was tested on stick models for kinematic correctness. Gleicher [21] interactively manipulated pre-existing key frames to synthesize new motion.

Many previous studies focused on editing motion to control the walking direction, and a few employed numerical methods to edit motion by considering direction as one abstraction [22]. Ling et al. [23] proposed to control over walk direction using deep learning, combining data driven autoencoders and deep reinforcement to enable the controllers.

Pavllo et al. [24] also adopted deep learning networks to model human motion, using convolution and recurrent networks for short and long term data synthesis, respectively. They adopted a strategy to penalize position errors rather than orientations errors while training the models.

All studies discussed in this section assumed that knee and elbow joints had single DoF. However, current state-of-the-art IMU motion capture systems cannot generate data conforming to this kinematic constraint, because elbow joints are not actually simple hinge joints but combine the radius and ulna joints [25]. The radius joint is responsible for forearm pronation and supination with approximately 180° range of motion (ROM); whereas the ulna is responsible for forearm extension and flexion. Thus, the elbow joint collectively exhibits two DoFs. The current study explicitly considers this detail when editing SHMD.

III. MOTION-SPHERE

It is important to understand the Motion-sphere tool [11]. Motion-sphere is an intuitive grid mapped unit sphere that represents swing as trajectory and twist as color coded beads or miniature models. The sphere is UV mapped with a grid texture, where each cell on the grid represents $10^\circ \times 10^\circ$. The grid acts as a scale to show swing extent in vertical and lateral directions. Labels Front, Right, Left, and Back on the grid provide bone segment direction relative to its parent segment. Orientation visualized in Motion-sphere is always with reference to the attention pose, where all limbs point south of sphere and the pelvis, chest, and head point north.

It is a standard procedure to decompose humanoid joint–bone movement defined by a quaternion (q) into twist (q_t) motion around an axis parallel to the bone axis and swing (q_s) motion around a specific axis [26]. Twist–swing decomposition considers joint–bone movement in twist first and swing next order, i.e., $(q = q_s q_t)$. Therefore, bone axis $\hat{v}$ could be constant. Thus, twist–swing decomposition can be expressed as

$$\hat{w} = q\hat{v}q^{-1}, \tag{1}$$

$$q_s = \left\{ cos\left(\frac{\alpha}{2}\right), \hat{u}sin\left(\frac{\alpha}{2}\right) \right\}, \tag{2}$$

and

$$q_t = q_s^{-1} q \tag{3}$$

where $\alpha = cos^{-1}(\hat{v} \cdot \hat{w})$; $\hat{u} = \hat{v} \times \hat{w}$; $\hat{w}(x, y, z) = q\hat{v}q^{-1} = q_s\hat{v}q_s^{-1}$; and there is a twist rotation around bone axis $(\hat{v})$ defined by quaternion q_t.

IV. Editing Sensor Acquired Human Motion Data

Twist and swing in SHMD depends on IMU placement on the body. SHMD will have non-zero orientation for all the three rotational DoFs, regardless of the bone being measured. We propose a two-step approach to edit SHMD to conform with human body kinematics.

Figure 2 visualizes KCA (highlighted areas) and KUA (darkened areas) for different human bone segments. Trajectories representing motion for a given segment should strictly be within the bone segment KCA. Motion-sphere labels left, right, front, and back indicate direction relative to the parent segment (See section III). Figure 2(b) shows that lower arms have single DoF about the ulna and therefore very small area they operate in front of upper arm, and the lower leg similarly has single DoF about the knee joint behind the upper leg (Fig. 2(e)). Upper arms and legs have ball socket joints, hence 3 DoFs, and can operate depending on individual flexibility. Motion-sphere provides the analyst with control to decide what specific flexibility should be applied.

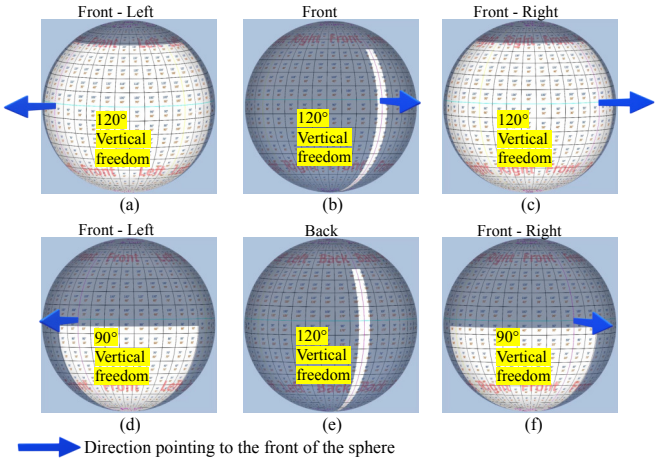

Fig. 2. Kinematic constrained areas (KCAs) and Kinematic unconstrained areas (KUAs) for (a) left upper arm, (b) lower arms (left and right), (c) right upper arm, (d) left upper leg, (e) lower legs (left and right), and (f) Right upper leg.

A. Latitude–Longitude Decomposition of $\hat{w}$

Consider left lower limb movement for example (Fig. 3 (a)). Lower leg lateral swing is synchronized with upper leg twist, but has independent vertical swing. Blue and red leg models have clockwise and anti-clockwise twist, respectively, with reference to the green leg model. However, the lower leg still swings behind the upper leg within the highlighted Motion-sphere KCA.

Figure 3(f) shows that SHMD implies 35° lateral swing in b_9 and 45° twist in b_8 (Fig 3(e)). Thus, b_8 is out of sync with b_9 by $-10°$. We apply the following steps for $[b_8, b_9]$, $[b_6,b_7]$, $[b_2,b_3]$, and $[b_4,b_5]$ pairs to edit SHMD for kinematic correctness.

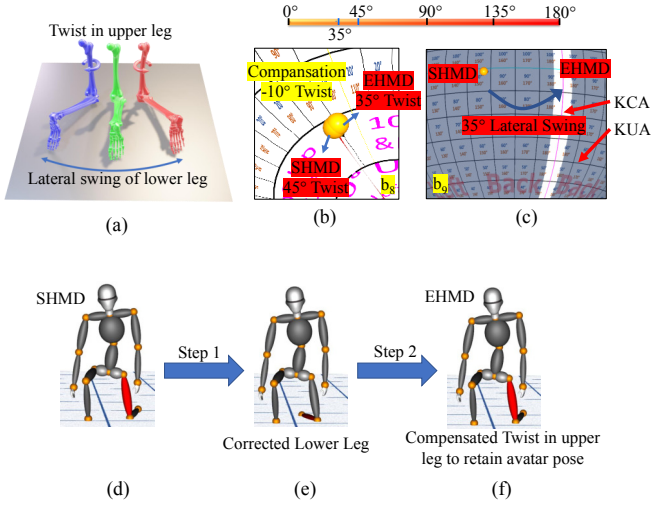

Fig. 3. Editing procedure for sensor acquired human motion data for b_9 relative to b_8: (a) Lower leg lateral swing due to upper leg twist, (b) left upper leg visualization with SHMD and EHMD exhibiting different twist, (c) left lower leg visualization with SHMD and EHMD exhibiting 35°swing differences (d) SHMD reconstruction on 3D avatar, (e) negating lateral swing in b_9, (f) compensating twist in b_8 to match the pose,

1) Negate lower leg lateral swing relative to the upper leg (35° in this example) and
2) compensate the negated swing from step 1 by adding upper leg twist ($-10°$ in this example),

which can be expressed as

$$\phi = arctan\left(\frac{y}{x}\right) \tag{4}$$

$$\theta = arctan\left(\frac{\sqrt{x^2 + y^2}}{z}\right), \tag{5}$$

Where ϕ is vertical swing and θ is lateral swing for the given $\hat{w}$.

Equations 4 and 5 decompose lateral swing for a given $\hat{w}$ into vertical and lateral swings, hence EHMD for the target bone segment (b_3, b_5, b_7 & b_9) is

$$q^{EHMD} = (sin(\theta), zcos(\theta)) \times q^{SHMD} \tag{6}$$

where the lateral swing according to the body frame is in the $z - axis$. Thus, EHMD for the corresponding parent segments (b_2, b_4, b_6, and b_8) can be expressed as

$$q^{EHMD}(p) = (sin(\delta), ycos(\delta)) \times q_t^{SHMD}(p), \tag{7}$$

where $\delta = acos(w) - \theta$ and $q_t^{SHMD}(p) = \{w, x, y, z\}$.

Figures 3(b) and (d) show there is no noticeable change to the avatar's pose since the editing process modifies twist in the kinematic chain to retain the pose, and that twist is not noticeable because the avatar is a stick model comprising parametric ellipsoids. The modified motion significantly changes underlying data that represents the pose in the Motion-sphere visualization.

B. Visualizing limiting joint movement

Upper arms and upper legs are attached to ball-socket joints, and hence have 3 DoFs rotation. However, rotation is limited laterally and vertically due to occlusion with other body parts and individual flexibility, and these limitations typically vary from person to person. We propose to extend Motion-sphere to visualize these human joint limitations.

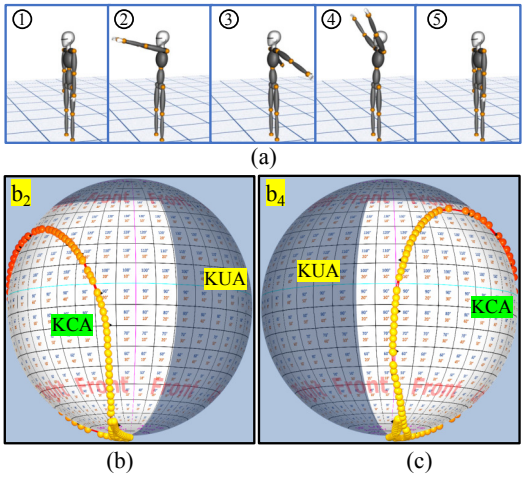

Fig. 4. (a) Upper hand forward rotation from TotalCapture [16] range of motion (ROM) data, and corresponding (b) right and (c) left upper arm kinematic constrained areas (KCAs)

Figures 4(b) and (c) shows forward rotation for the right and left upper arms, respectively, from key frames 1–5. The spheres visualizes the upper arms, with darkened area indicating where the upper arm cannot move.

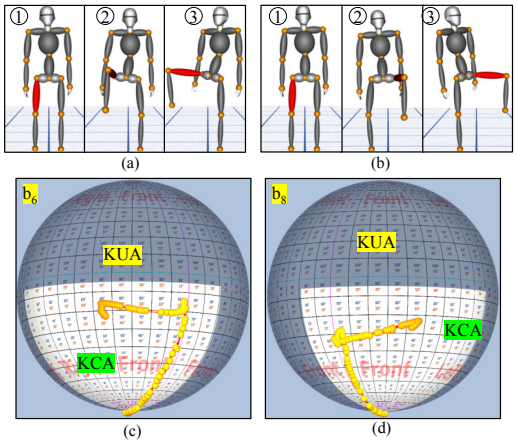

Fig. 5. (a) Right upper leg and (b) left upper leg forward–lateral rotation data in TotalCapture [16] range of motion (ROM) data; and corresponding (c) right and (d) left kinematic constrained areas (KCAs)

Figures 5(a) and (b) show forward and lateral rotation for right and left legs, respectively, from key frames 1–3. The right upper leg has more freedom towards the right, whereas the left upper leg has more freedom of movement to the left of the pelvis, indicated by labels on the sphere texture. Both legs move freely within their respective KCAs but cannot kinematically rotate into the KUAs. As discussed above, these limitations are specific to each individual, where those with more flexible body may have increased KCA range and/or decreased KUA. Motion-sphere provides controls to modify KCAs and KUAs according to the specific scenario.

V. Results

This section compares various poses SHMD and EHMD data. We then consider a walk scenario to demonstrate the effect on joint position estimation.

A. EHMD effects on reconstruction and orientation

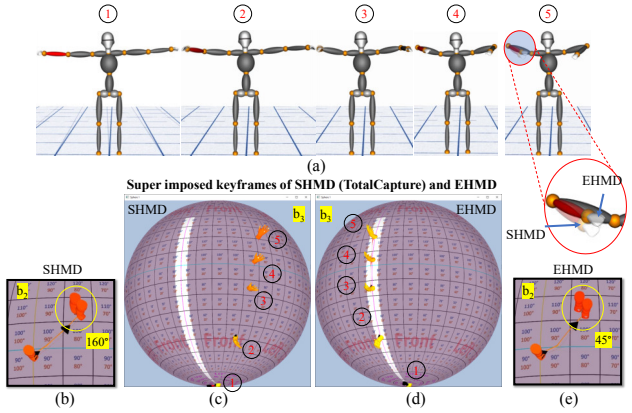

Fig. 6. TotalCapture dataset range of motion (ROM) sequence for bending the lower arm from T-pose: (a) superimposed SHMD and EHMD key frames, (b) SHMD right upper arm visualization with 160° twist, (c) SMHD right lower arm swing falls into kinematic unconstrained area (KUA) (d) EHMD right lower arm motion with kinematically correct orientation, and (e) EHMD right upper hand with kinematically corrected twist.

Figure 6 shows how lateral movement in the right lower arm is negated and a corresponding twist introduced in the upper arm to match the key poses. Key frame 5 shows 160° twist (supination) in the arm, whereas the radius can only achieve 90° pronation and 90° supination. The EHMD corrected pose only requires 45° twist.

Figure 7(a) shows 6 key frames from the TotalCapture ROM dataset for the right leg. The lower leg exhibits a swing back and slightly to the left, moving outside the KCA (Fig. 7(d)). EHMD negates this lateral swing, compensating with an upper leg twist (Figs. 7(e)).

Figure 8(a) shows right upper leg forward motion followed by lateral motion. The Motion-sphere visualization depicts key poses with respect to the attention pose. Lateral swing inherently adds twist in the bone segment (Fig. 8(b) and (c)), with approximately 35° swing in the lower leg (Fig. 8(d)). However the lower leg positions on the Motion-sphere is outside the KCA. Figure 8(e) shows the corresponding EHMD for the lower leg. Lateral movement is fully negated, twist in the lower leg = 0° and twist is added to the upper leg (Fig 8(c)).

B. EHMD effect on position estimation

We used a vector based position estimation technique [9] to compare between SHMD and EHMD against ground truth

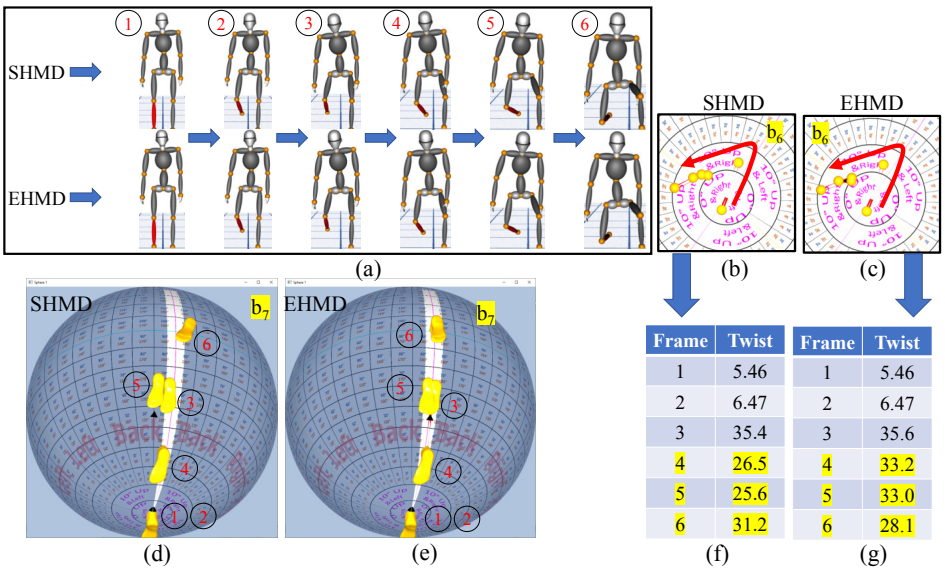

Frame	Twist
1	5.46
2	6.47
3	35.4
4	26.5
5	25.6
6	31.2

Frame	Twist
1	5.46
2	6.47
3	35.6
4	33.2
5	33.0
6	28.1

Fig. 7. TotalCapture range of motion (ROM) dataset sequence for lunge motion from attention pose reconstructed on 3D avatar: (a) SHMD and EHMD keyframes 1—6; (b) SHMD and (c) EHMD for right upper leg; (d) SHMD and (e) EHMD (with kinematically corrected orientation) for right lower leg; (f) SHMD and (g) EHMD twist for right upper leg.

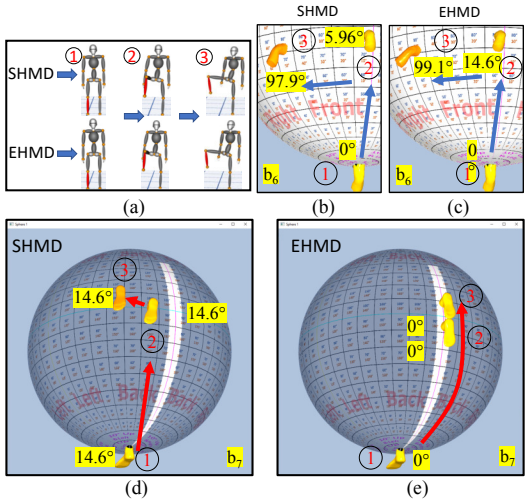

Fig. 8. (a) Three key frames showing right lower leg movement, (b) SHMD key poses and (c) EHMD with corrected twists for right upper leg movement; (d) SHMD and (e) EHMD with kinematically corrected twist for right lower leg movement.

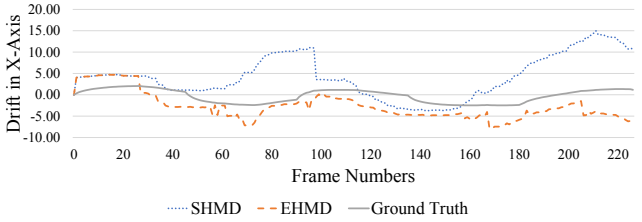

Fig. 9. SHMD and EHMD with respect to ground truth data for walk scenario. Kinematically incorrect lower leg lateral swing (SHMD) caused the virtual avatar to drift to one side, which was significantly corrected by the proposed approach (EHMD)

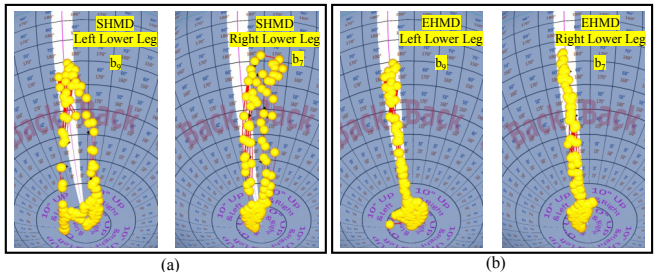

Fig. 10. Motion-sphere visualization for SHMD and EHMD: (a) SHMD of left and right lower leg (b_9 and b_7) and (b) EHMD of left anf right lower leg (b_9 and b_7)

for a walk scenario, measuring pelvis position during the entire motion. The ground truth data is that of the the TotalCapture data set which is acquired from the state-of-the-art image based motion capture system called Vicon. The vector based approach exhibited ± 5 cm average drift against TotalCapture dataset ground truth. Figure 9 shows that corrected orientations using the proposed technique achieved ± 3 cm average drift.

Lateral swing in the lower legs for SHMD foot position greatly affected lateral positioning, drifting the avatar towards one side; whereas EHMD negated this lateral swing and greatly reduced position drift. Figure 10 shows Motion-sphere visualizations for the lower legs.

C. Application on Motion-Capture in real time

We evaluated the proposed method by capturing the positions of pelvis and right foot over time against the data from the Disto meter. The user performed an activity requiring position movement in the pelvis and right leg; walking from the start position, sitting on the chair, and then moving to a small table and placing their right foot on the table. The RMSE relative to ground truth, for the pelvis is

2.82 cm and for foot is 2.42 cm [27].

VI. Discussion and Conclusion

This paper proposed editing sensor acquired human motion data for kinematic correctness. Correcting sensor data to adhere to human body kinematics is a multi-dimensional optimization problem, where all participating joints need to be considered. Limbs (both upper and lower) play a major role in human locomotion and robotics applications. Therefore, We focused on elbow and knee joint kinematics to demonstrate the concept, using the Motion-sphere intuitive visual analytic tool for editing. The nature of the research is exploratory. Therefore we intend to validate the proposed method for other movement types in future research. Editing all sensor captured data is laborious and time consuming, hence animators generally edit selected key frames and interpolate rotation and position between them. For instance Blender (www.blender.org) includes constant, linear, Bezier, sinusoidal, quadratic, cubic, quartic, expontial, and circular interpolation options.

Many existing state-of-the-art editing systems including Blender, and 3D Max twist the hand instead of forearm for pronation and supination movements. Therefore the elbow joint has 2 DOF in the proposed system as opposed to 1 DOF considered in the literature.

Similar to most motion editing tools, Motion-sphere is extended to include key frame selection, enabling the analyst to make informed decisions about key frames selected for editing, and also the number of intermediate key frames. Motion-sphere implements spherical linear interpolation to synthesize motion. This study . Our results confirms that proposed method does not affect motion reconstruction visually, but improves joint position estimation.

However diligently key frames are chosen, edited, and synthesized, the selection introduces artifacts in the resulting motion. Therefore, a robust technique to edit human motion holistically is essential. Thus, future work will explore deep learning models to edit and synthesize human motion to be free from artifacts.

ACKNOWLEDGMENT

This work was supported by Institute of Information & Communications Technology Planning & Evaluation (IITP) grant funded by the Korea government (MSIT) (No. 2018-0-00599, SW Computing Industry Source Technology Development Project, SW Star Lab).

References

[1] Liu, Y.; Zang, X.; Heng, S.; Lin, Z.; Zhao, J. Human-like walking with heel off and toe support for biped robot. Appl. Sci. 2017, 7, 499. https://doi.org/10.3390/app7050499

[2] Carbone, G.; Gerding, E.C.; Corves, B.; Cafolla, D.; Russo, M.; Ceccarelli, M. Design of a two-DOFs driving mechanism for a motion-assisted finger exoskeleton. Appl. Sci. 2020, 10, 2619. https://doi.org/10.3390/app10072619.

[3] Ren, B.; Luo, X.; Chen, J. Single leg gait tracking of lower limb exoskeleton based on adaptive iterative learning control. Appl. Sci. 2019, 9, 2251. https://doi.org/10.3390/app9112251.

[4] Seel, T.; Raisch, J.; Schauer, T. IMU-based joint angle measurement for gait analysis. Sensors 2014, 14, 6891–6909. https://doi.org/10.3390/s140406891.

[5] Cheng, P., & Oelmann, B. Joint-angle measurement using accelerometers and gyroscopes: A survey. IEEE Trans. Instr. Meas. 2009, 59(2), 404–414.

[6] Takeda, R., Tadano, S., Natorigawa, A., Todoh, M., & Yoshinari, S. Gait posture estimation using wearable acceleration and gyro sensors. J. Biomech. 2009, 42(15), 2486–2494.

[7] Favre, J., Jolles, B. M., Aissaoui, R., & Aminian, K. Ambulatory measurement of 3D knee joint angle. J. Biomech. 2008, 41(5), 1029–1035.

[8] Roetenberg, D., Luinge, H., & Slycke, P. Xsens MVN: Full 6 DoF human motion tracking using miniature inertial sensors. Xsens Motion Technologies BV 2009, Tech. Rep. 1.

[9] Patil, A.K.; Balasubramanyam, A.; Ryu, J.Y.; B N, P.K.; Chakravarthi, B.; Chai, Y.H. Fusion of multiple lidars and inertial sensors for the real-time pose tracking of human motion. Sensors 2020, 20, 5342. https://doi.org/10.3390/s20185342

[10] Cheng, P., & Oelmann, B. Joint-angle measurement using accelerometers and gyroscopes: A survey. IEEE Trans. Instr. Meas. 2009, 59(2), 404–414.

[11] Balasubramanyam, A.; Patil, A.K.; Chakravarthi, B.; Ryu, J.Y.; Chai, Y.H. Motion-sphere: Visual representation of the subtle motion of human joints. Appl. Sci. 2020, 10, 6462. https://doi.org/10.3390/app10186462.

[12] Li, W., Bartram, L., & Pasquier, P. Techniques and approaches in static visualization of motion capture data. In Proceedings of the 3rd International Symposium on Movement and Computing 2016, 1–8.

[13] Bouvier-Zappa, S., Ostromoukhov, V., & Poulin, P. Motion cues for illustration of skeletal motion capture data. In Proceedings of the 5th International Symposium on Non-photorealistic Animation and Rendering 2007, 133–140).

[14] Cutting, J. E. Representing motion in a static image: constraints and parallels in art, science, and popular culture. Perception 2002, 31(10), 1165–1193.

[15] Hu, Y., Wu, S., Xia, S., Fu, J., & Chen, W. Motion track: Visualizing variations of human motion data. In 2010 IEEE Pacific Visualization Symposium (PacificVis) 2010, 153–160.

[16] Trumble, M., Gilbert, A., Malleson, C., Hilton, A., & Collomosse, J. P. (2017, September). TotalCapture: 3D human pose estimation fusing video and inertial sensors. In BMVC [R27]2017, 2(5), 1–13).

[17] Hernández, J., Cabido, R., Montemayor, A. S., & Pantrigo, J. J. (2014). Human activity recognition based on kinematic features. Expert Systems, 31(4), 345-353.

[18] Wang, X., Chen, Q., & Wang, W. 3D human motion editing and synthesis: A survey. Comp. Math. Methods Med., 2014 <volume, pages>.

[19] Kovar, L., Schreiner, J., & Gleicher, M. Footskate cleanup for motion capture editing. In Proceedings of the 2002 ACM SIGGRAPH/Eurographics Symposium on Computer animation 2002, 97–104.

[20] Lee, J., & Shin, S. Y. A hierarchical approach to interactive motion editing for human-like figures. In Proceedings of the 26th Annual Conference on Computer Graphics and Interactive Techniques 1999, 39–48.

[21] Gleicher, M. Motion editing with spacetime constraints. In Proceedings of the 1997 Symposium on Interactive 3D Graphics 1997, 139–ff.

[22] Gleicher, M. Motion path editing. In Proceedings of the 2001 Symposium on Interactive 3D Graphics 2001, 195–202.

[23] Ling, H. Y., Zinno, F., Cheng, G., & Van De Panne, M. Character controllers using motion vaes[R30]. ACM Trans. Graph. (TOG) 2002, 39(4), 40–41.

[24] Pavllo, D., Feichtenhofer, C., Auli, M., & Grangier, D. Modeling human motion with quaternion-based neural networks. Int. J. Comp. Vis. 2019, <volume>[R31], 1–18.

[25] Mansfield, P. J., & Neumann, D. A. Essentials of kinesiology for the physical therapist assistant e-book. Elsevier Health Sciences, 2018.

[26] Dobrowolski, P. Swing-twist decomposition in Clifford algebra. 2015, arXiv preprint arXiv:1506.05481.

[27] Patil AK, Balasubramanyam A, Ryu JY, Chakravarthi B, Chai YH. An Open-Source Platform for Human Pose Estimation and Tracking Using a Heterogeneous Multi-Sensor System. Sensors. 2021; 21(7):2340.